

Particle-Size Analysis in Mass Crystallization from Solutions

G. Zelmanov and R. Semiat

Chemical Engineering Dept., Technion, Israel Institute for Technology, Technion City,
Haifa 32000, Israel

The problem of product-size distribution exiting a crystallizer is addressed theoretically and experimentally. The distribution function of the particle size is solved and demonstrated experimentally as a function of fines destruction, solids content of feed, particle circulation ratio, feed particle sizes, particle concentration. Theoretical tools are given for estimation of various important parameters such as distribution moments, rate of growth, rate of nuclei production and particle-size distribution. A good agreement is shown between the theoretical model and the experimental results.

Introduction

Control of particle-size distribution in the operation of continuous crystallizers is of extreme importance in theory and practice. Different types of concentrated slurries, as well as dry and wet solid streams, flow into such production systems from highly concentrated product flowing to filters, through diluted, low concentrated slurries, circulated for destruction purposes, and wet solids for drying followed dry powders toward packaging. Data on the particle-size distribution of the particles is needed.

Saeman (1956) derived the relationships of the crystal-size distribution in a single-tank, continuous mixed suspension crystallizer, for different operating parameters. A solution was also given for separate cases of mixed and classified products removed from the crystallizer. It was shown that the theoretical predictions of the size distribution were in reasonable agreement with results of a large commercial crystallizing unit. The extreme influence of nucleation rate on resulting size distributions was emphasized in this work.

Han and Shinnar (1968) investigated the steady-state behavior of a crystallizer with a classified product removal. It has been assumed previously that the growth rate and the nucleation rate of the particles are functions of the supersaturation, and are independent of the volume and the nature of the crystal magma. The developed method for obtaining particle-size distributions was based on the use of residence time distribution. The effect of classification on the crystal-

lizer's performance was discussed with the help of some illustrative examples. It has already been shown that, in order to increase the average particle size, it is most important to reduce the nucleation rate.

Nauman and Szabo (1971a,b) studied the crystal-size distribution and steady-state operation characteristic of the continuous-recycle crystallizers, which have an internal fines trap. The approach to the problem was based on a classical crystallization theory, namely steady-state operation and growth rate independent of crystal size. Nonselective and selective fines destruction in recycled crystallizers were also considered. The researchers demonstrated that a selective fines trap can have a dramatic improvement in the crystallizer performance.

Randolph and Larson (1988) formulated a general population balance for particles in an arbitrary suspension. The classical model for a crystal-size distribution was obtained. Equations have been formulated for growth and nucleation of particles in both continuous and batch operations. The population balance was expressed in the number-volume and mass-size coordinate systems. Mass-conserving the "birth" and "death" functions were also formulated. In some cases, the most efficient method of the solution of particle-size equations was to solve the moment equations and then to recover the particle-size distribution from the moments.

Rawlings et al. (1993) reviewed and discussed the modeling of the crystal quality (size, shape, and purity) and the control of crystallization processes. The review focused on model development, model solution, measurement techniques, parameter estimation, and size control.

Correspondence concerning this article should be addressed to R. Semiat.

Rojkowski (1993) showed that the population balance in a mixed suspension crystallizer with a mixed product removal can be transformed in the case of constant (initial) crystal growth rate dispersion mechanism, into a form similar to a size-dependent growth rate mechanism. This allows to interpret the experimental crystal-size distribution data resulting from the dispersion in terms of size-dependent mean growth rate.

Rawling and Ray (1987a,b) developed a class of simplified polymerization models. These models include the distribution of particle size, radical numbers, and the coupling of the particle initiation rate to the particle-size distribution. An analytical solution to the modeling equations was found. Necessary and sufficient conditions for local stability were derived.

A direct optimization method to estimate nucleation and crystal growth rate parameters from seeded batch cooling crystallization experiments was evaluated by Qiu and Rasmussen (1994). Parameters in kinetic equations were determined by the nonlinear optimization of a dynamic model of the experiment. The optimization objective function includes both the solution concentration and the product-size distribution data.

Hounslow and Wynn (1992) and Wynn and Hounslow (1996) described an alternative and a new approach in the form of integral equations. The general integral equations were simplified for more specific cases. They also suggested new solution strategies for simulating the particle-size distribution in practice. An industrial case simulating the startup of two crystallizers in series was studied and presented in detail.

Eek et al. (1995) developed a model for the dynamics of a single-stage suspension crystallizer. A population balance for the dynamics of the crystal-size distribution with mass and heat balances was described. Crystal-size distribution dynamics data was obtained from the startup experiments with a pilot plant operated at different process conditions. A nonlinear parameter estimation procedure determined the empirical parameters directly from the raw sensor data.

Several empirical relations are presented in the literature for the classification function (Tavare, 1995; Randolph and Larson, 1988). The idealized description was given by Saeiman (1956) and Han and Shinnar (1968). Randolph and Larson (1988) presented the so-called R-Z crystallizer model and showed that internal fines separation and destruction can be used to alter a crystal-size distribution function. For an efficient classifier, the classification function may be approximated by a step function (Han and Shinnar, 1968; Todes et al., 1984).

The purpose of the present work was to build a tool that would be used to estimate the efficiency of the different production methods by studying the influence of the different crystallization parameters on the size distribution of the product. The crystallizer studied here is the continuous single-stage draft-tube baffled (DTB) crystallizer equipped with a classified fines removal system and a fines dissolver.

In order to analyze crystallization processes from salt solutions some simplifying assumptions are needed: consider the crystallizer as a perfect-mixed system operated at a steady state with lumped parameters; all particles grow under identical conditions, where the averaged characteristic of the examined process may be used. These assumptions have been

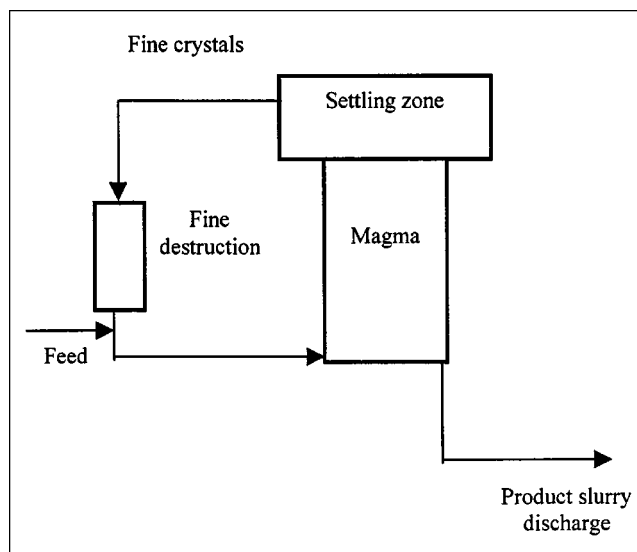


Figure 1. Simple crystallizer with circulation and fines destruction.

widely accepted in the literature. The separated fines are dissolved by heating or by dilution of the fines slurry flow. For simplification, all fines assumed to be dissolved.

By investigating feed containing crystals, mono-sized crystals were assumed, so that the size-distribution function of the feed crystals can be approximated by a delta function. Figure 1 represents a simple sketch of a common crystallizer with a circulation and fines destruction unit.

Crystallization with Fines Rejection

With the described assumptions, the equation for the size distribution function $f(x)$ of crystals of size x , for continuous crystallizer where selective discharge of fine crystals take place can be written in the form (Randolph and Larson, 1988)

$$G \frac{df(x)}{dx} = B\delta(x - x_0) - kf(x) - \chi f(x)\Theta(\alpha - x) \quad (1)$$

where B and G are the rates of formation and growth of new crystallization nuclei; x_0 is the initial nucleus size; k is the rate of crystals discharge from the crystallizer (1/S); χ is the rate of discharge of a stream of fine particles of size $x < \alpha$ (1/S); δ is the Dirac delta function; and Θ is the unit Heaviside function

$$\begin{aligned} \Theta(x - \alpha) &= 1, \quad \text{for } x > \alpha, \quad \text{and} \\ \Theta(x - \alpha) &= 0, \quad \text{for } x < \alpha. \end{aligned} \quad (2)$$

The solution of Eq. 1 with boundary condition $f(0) = 0$ can be written in the form

$$f(x) = \frac{B}{G} \exp\left(-\frac{k + \chi}{G}x\right) \quad (3)$$

for $x < \alpha$, and

$$f(x) = \frac{B}{G} \exp\left(-\frac{kx + \chi\alpha}{G}\right) \quad (4)$$

for $x > \alpha$.

By calculating the corresponding moments of the distribution function $f(x) - \mu(i)$, the number of particles N , salt output rate Q , volume of particles in the crystallizer V (m^3), and the average crystal size d (mm) can be determined

$$\mu(i) = \int_0^\infty x^i f(x) dx \quad (5)$$

$$N = \mu(0) \quad (6)$$

$$Q = 3\gamma G\mu(2) = 3\gamma G \int_0^\infty x^2 f(x) dx \quad (7)$$

$$V = \gamma\mu(3) \quad (8)$$

$$d = \frac{\mu(4)}{\mu(3)} \quad (9)$$

where γ is a shape factor.

Substituting the solution of Eq. 3 and Eq. 4 in Eq. 5, we obtain an equation for determining the moments of the distribution function $\mu(i)$

$$\mu(i) = \mu(i, x < \alpha) + \mu(i, x > \alpha) \quad (10)$$

where

$$\begin{aligned} \mu(i, x < \alpha) &= \int_0^\alpha x^i f(x) dx = \frac{B}{G} i! \exp\left(-\frac{k + \chi}{G} \alpha\right) * \\ &\left(\left(\frac{k + \chi}{G}\right)^{-(i+1)} \exp\left(\frac{k + \chi}{G} \alpha\right) - \sum_{j=0}^i \frac{\alpha^{i-j}}{(i-j)!} \left(\frac{k + \chi}{G}\right)^{-(j-1)} \right) \\ \mu(i, x > \alpha) &= \int_\alpha^\infty x^i f(x) dx = \frac{B}{G} i! \sum_{j=0}^i \frac{\alpha^{i-j}}{(i-j)!} \left(\frac{k}{G}\right)^{-(j+1)} \\ &\times \exp\left(-\frac{k + \chi}{G} \alpha\right) \end{aligned} \quad (11)$$

The larger size of fine particles α (m) discharged from a crystallizer, can be determined from Stock's equation, which agrees well with the experimental data (Todes et al., 1984). The solid-phase output rate Q (1/s) can be determined from the mass balance. The rate of formation of new crystallization nuclei B can be determined from the experimental data. The average size of crystals d , the rate of growth of crystal G , the rate of crystals discharge, and the other characteristics of the particle-size distribution of the solid phase may be calculated from the above system of Eqs. 7–11.

Figure 2 shows some theoretical calculations of the influence of the ratio of fine crystals output rate Q_1 , discharged from the crystallizer and destroyed, to solid-phase output rate Q (1/s), on the average-size distribution d , the rate of crystal growth G and number of crystals N within the crystallizer

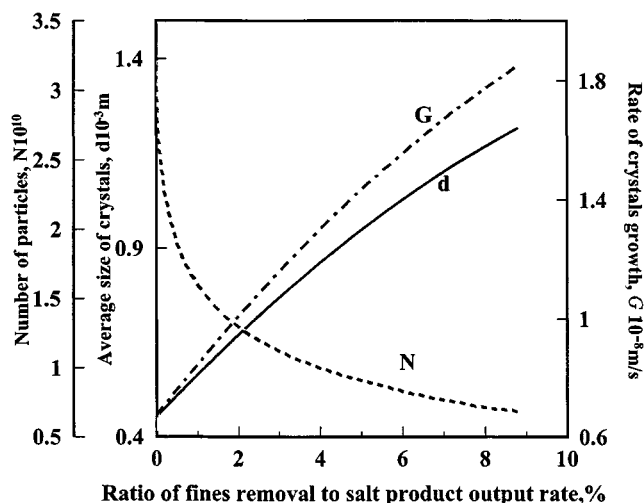


Figure 2. Theoretically calculated influence of relative rate of fine discharge and destruction on particle average size, rate of growth, and number of particles in the crystallizer.

($1/\text{m}^3$). Here, $\varphi_1 = Q_1/Q$ where Q_1 is the output rate of fine crystals from settling zone.

The output rate of the fine crystals from settler Q_1 may be calculated from Eq. 7. With rising dimensionless parameter φ_1 from 0 to about 9% under otherwise constant conditions, the average size of crystals d and the rate of crystals growth G (m/s) increases about threefold while the number of crystals in crystallizer N decreases by almost an order of magnitude.

This may be explained easily as follows: the rising of the dimensionless parameter φ_1 causes a decrease in the number of particles in the crystallizer. The supersaturation in the solution is relieved on a smaller number of particles, leading to the increase in the size of crystals and the rate of crystals growth G (Randolph and Larson, 1988). Therefore, by changing the output rate of the fine crystals from the settler Q_1 , it is possible to control and regulate the average size of crystals and size distribution function of the produced crystals.

Feed Containing Crystals

In some cases, a crystallizer is fed with a saturated stream containing solid particles having their own size distribution. This is also in the case where some crystals remained in the recirculation stream, and part or all of the recirculated crystals were not destroyed in the path. In order to estimate the influence of this flow and the average size of the feed crystals on the product particle-size distribution, the balance equation for the number of particles of size x was reconsidered. In this case, for simplicity, no small size destruction was assumed

$$G \frac{df(x)}{dx} = B\delta(x - x_0) - kf(x) + \kappa\phi(x) \quad (12)$$

where $\phi(x)$ is the size distribution function of the feed crystals ($1/\text{m}^4$), fed to the crystallizer and κ is the crystals' feed rate (1/s). Considering the mono-fraction distribution in this

case, the size distribution function $\phi(x)$ may be approximated by the expression

$$\phi(x) = \delta(x - R) \quad (13)$$

where R is the size of feed particles.

The solution of Eq. 12 with the boundary condition $f(0) = 0$ can be written in the form

$$f(x) = \frac{B}{G} \exp\left(-\frac{kx}{G}\right) \quad (14a)$$

for $x < R$, and

$$f(x) = \frac{B}{G} \exp\left(-\frac{kx}{G}\right) + \frac{\kappa}{G} \exp\left[-\frac{k}{G}(x - R)\right] \quad (14b)$$

for $x > R$.

By calculating the corresponding moments of the distribution function in Eqs. 12–14a and 14b, the number of particles N in a crystallizer can be determined, together with the crystal output rate Q , volume of crystals in crystallizer V , and average crystal size d .

$$N = \frac{B + \kappa}{k} \quad (15)$$

$$Q = 6\gamma \left(\frac{G}{k}\right)^3 \left[B + \kappa \sum_{i=0}^2 \frac{1}{i!} \left(\frac{kR}{G}\right)^i \right] \quad (16)$$

$$V = 6 \frac{\gamma}{k} \left(\frac{G}{k}\right)^3 \left[B + \kappa \sum_{i=0}^3 \frac{1}{i!} \left(\frac{kR}{G}\right)^i \right] \quad (17)$$

$$d = 8 \left(\frac{G}{k}\right) \frac{B + \kappa \sum_{i=0}^4 \frac{1}{i!} \left(\frac{kR}{G}\right)^i}{B + \kappa \sum_{i=0}^3 \frac{1}{i!} \left(\frac{kR}{G}\right)^i} \quad (18)$$

Comparison between Feed Containing and Noncontaining Crystals

For a simple estimation of the flux and the size of feed crystals influence on the product particles-size distribution, the expression for the number-average crystals size- l may be considered

$$l = \frac{\mu(1)}{N} \quad (9a)$$

where $\mu(1)$ and the number of particles N may be determined from expressions 5 and 6. In the case of solids fed into the crystallizer, an expression for l_R may be defined, for the number-average of the product crystal size

$$l_R = \frac{G}{k} + \frac{\kappa^*}{1 + \kappa^*} R \quad (19)$$

where $k^* = \kappa/B$.

Equation 16 for calculating the solid-phase output rate Q can be rewritten as

$$I^*{}^3 = (G/k)^3 \left[1 + \kappa^* \sum_{i=0}^2 \frac{1}{i!} \left(\frac{kR}{G}\right)^i \right] \quad (20)$$

where $I^* = (Q/6\gamma B)^{1/3}$ is the average crystal size with no solid feed.

From Eqs. 19 and 20

$$l_R = \frac{I^*}{\left[1 + \kappa^* \sum_{i=0}^2 \frac{1}{i!} \left(\frac{kR}{G}\right)^i \right]^{1/3}} + \frac{\kappa^*}{1 + \kappa^*} R \quad (21)$$

As in practical cases, a condition

$$\kappa^* \sum_{i=0}^2 \frac{1}{i!} \left(\frac{kR}{G}\right)^i < 1$$

is satisfied, simplified by the Taylor series yields

$$l_R - I^* = \frac{\kappa^*}{1 + \kappa^*} R - \frac{1}{3} I^* \kappa^* \sum_{i=0}^2 \frac{1}{i!} \left(\frac{kR}{G}\right)^i \quad (22)$$

Comparing the expressions for calculation of the average crystal size without (I^*) and with solid feed (l_R), it is possible to show a condition from Eq. 22

$$\frac{1}{3} I^* \sum_{i=0}^2 \frac{1}{i!} \left(\frac{kR}{G}\right)^i < \frac{R}{1 + \kappa^*} \quad (23)$$

which gives a coarser product with crystals solid feed, whereas if

$$\frac{1}{3} I^* \sum_{i=0}^2 \frac{1}{i!} \left(\frac{kR}{G}\right)^i > \frac{R}{1 + \kappa^*} \quad (24)$$

feeding solids results in finer crystals in the product.

Examination of the results shows that the particle size R (m or mm) of the feed crystals has a significant influence on the particle-size distribution of the final product. This can be explained in the following paragraph. The flux of solid feed q (m³/s) can be written as $q = \gamma \kappa R^3$, or

$$\kappa = \frac{q}{\gamma R^3} \quad (25)$$

A value of R^* can be determined in the case where no influence exists when particles are fed

$$\frac{1}{3} I^* \sum_{i=0}^2 \frac{1}{i!} \left(\frac{kR^*}{G}\right)^i = \frac{R^*}{1 + \kappa^*} \quad (26)$$

Introduction of finer crystals with size $R < R^*$ under otherwise constant conditions increases the total number of particles, and, hence, increases the value of κ^* . The supersaturation within the solution is relieved of a larger number of par-

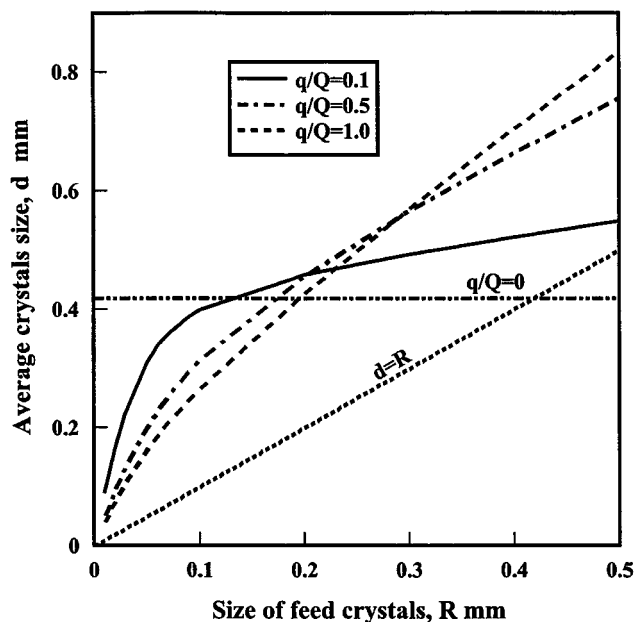


Figure 3. Theoretical dependence of crystals average size on the average size of the crystals in feed for different solid feeds to product ratios.

ticles, which leads to a decrease of the grain size I_R (Q and q are constant). Further increase of the size of the feed crystals R leads to a decrease in the number of particles. The supersaturation within the solution is relieved of a smaller number of particles, and this leads to an increase of the grain size I_R . The value of R^* can be determined from the relation (Eqs. 22 and 26) $I_R = I^*$.

Figure 3 shows theoretical calculations of the influence of the size R , and the dimensionless parameter φ , where $\varphi = q/Q$ on the average crystals size d . The horizontal line presents a case where no solids were fed into the crystallizer. This is independent of the average size of the feed crystals. This line intersects with other lines at a point corresponding to the values of R^* for different values of φ . The product's average crystal size is increased above this line, as R increases, but reduces below the line as R decreases. Increasing the value of φ , for the same value of R , causes further increase of the average size, while the opposite is the case for low values of R .

Experimental Studies

A unit of a draft-tube agitated crystallizer with a dual circulation circuit (DTB) for vacuum-crystallization (Zelmanov et al., 1979, 1988, 1991) of 0.017 m³ capacity was used for experimental studies of potassium chloride controlled vacuum-crystallization. The crystallizer with the feed and product streams is given Figure 4.

In these experiments the following factors were varied under otherwise constant conditions:

- The volume of particles in the crystallizer— V
- The suspension circulation to magma volume ratio— ω
- The size of feed particles— R
- The flux of the solid feed— q
- The solid phase output rate— Q .

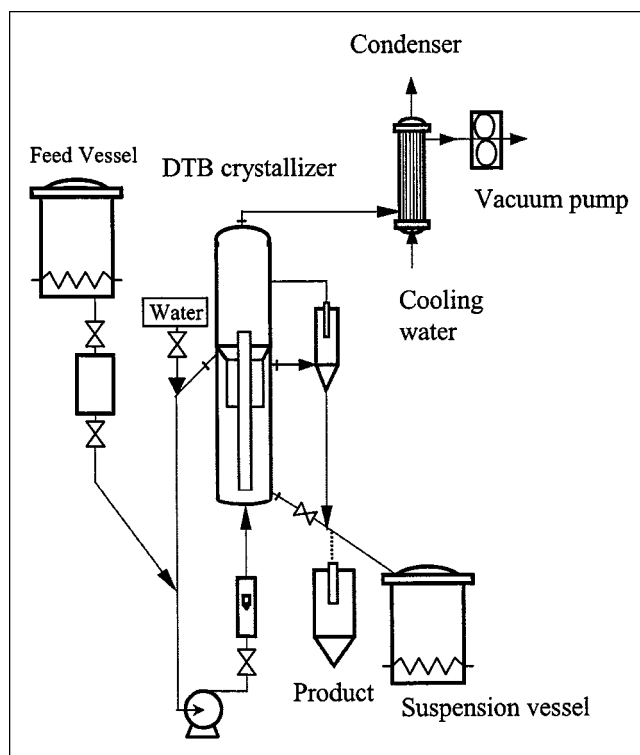


Figure 4. Experimental system.

In order to maintain the specified regime and to monitor the performance of the apparatus, the following quantities or values were measured and calculated during the experiments:

- Flow rate, temperature, and concentration (density) of the feed solution;
- Temperature and concentration (density) of the mother liquor; and
- The particle-size distribution of product and average crystal size- d .

The solid-phase output rate- Q can be determined from the mass balance. The rate of formation of new crystallization nuclei B , the rate of crystals growth G , and the rate of crystals discharge from crystallizer k were determined from the values of the salt output rate Q . The volume of solid phase V , and average crystal size d were found by evaluation of experimental data with the aid of the system of Eqs. 7–9

$$Q = kV + \chi V_1(B, G, k) \quad (27)$$

$$V = V(B, G, k) \quad (28)$$

$$d = d(G, k) \quad (29)$$

where

$$V_1(B, G, k) = \gamma\mu(3, x < \alpha) \quad (30)$$

$$V = \gamma\mu(3) \quad (31)$$

$$d = \frac{\mu(4)}{\mu(3)} \quad (32)$$

V_1 represents the volume of crystals in the settling zone where $x < \alpha$.

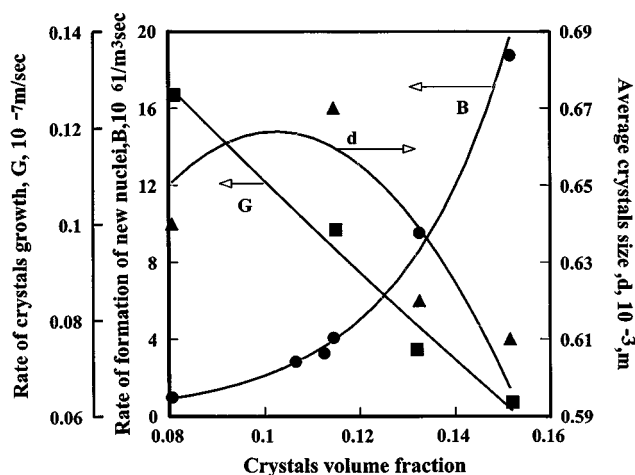


Figure 5. Rate formation of KCl new nuclei, average crystals size and rate of crystal growth as function of crystals volume fraction.

The dots represent experimental data; the lines are calculated theoretical results; ● = rate of formation of new nuclei, B; ■ = rate of crystal growth G; ▲ = average crystal size d.

Controlled Crystallization of KCl

The experimental conditions that were kept during the experiments:

- clear solution feed flow rate $0.33 \cdot 10^{-5} \text{ m}^3/\text{s}$,
- temperature of suspension in crystallizer $16\text{--}20^\circ\text{C}$,
- concentration of mother liquor $25.3\text{--}25.7\%$ KCl,
- density of mother liquor $1,173\text{--}1,175 \text{ kg}/\text{m}^3$;
- Constant suspension circulation to magma volume ratio with constant rate of fines destruction.

The results of these investigations are given in Figures 5 to 8. The dots represent experimental data and lines are theo-

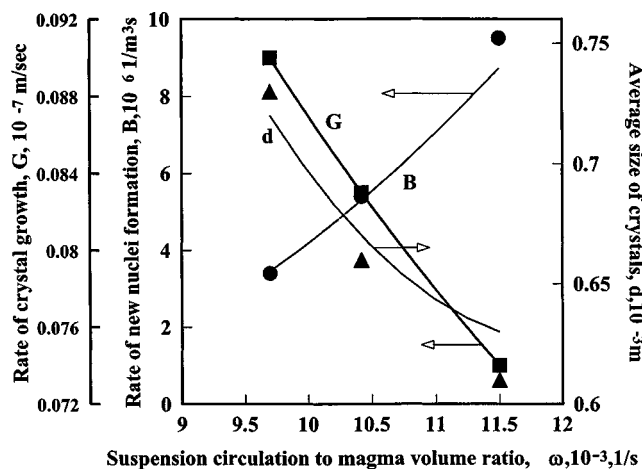


Figure 6. Influence of suspension circulation to magma volume ratio on the rate of crystals growth and on crystals sizes.

The dots represent experimental data; the lines are calculated theoretical results; ● = rate of formation of new nuclei B; ■ = rate of crystal growth G; ▲ = average crystal size d.

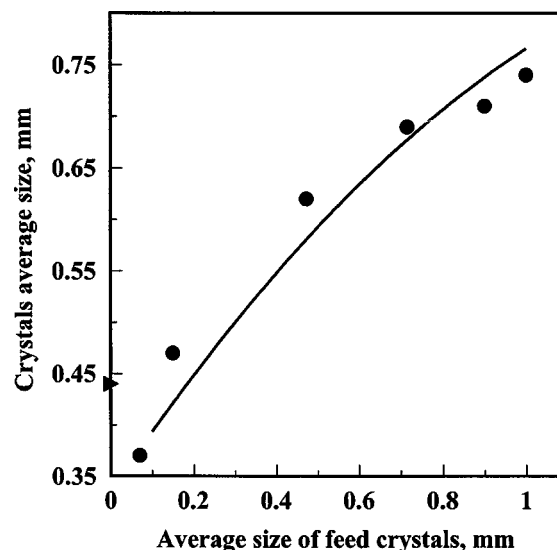


Figure 7. Dependence of the produced crystals size on the average size of the feed crystals.

The dots represent experimental data; the lines are calculated theoretical results. The triangle is related to the case of no initial crystals feed.

retically calculated results, based on the equations above. On examination, these results show that the rate of formation of new crystallization nuclei B increases almost by a factor of 20 with a change of approx. 100% in the crystals volume concentration within the crystallizer. This was obtained both experimentally and theoretically, as shown in Figure 5. The rate of crystals' growth G decreases by about 50%. The average size of the crystals is increased first with the increase of the internal crystals volume concentration within the crystallizer, and then reduced. Based on the small changes in the average

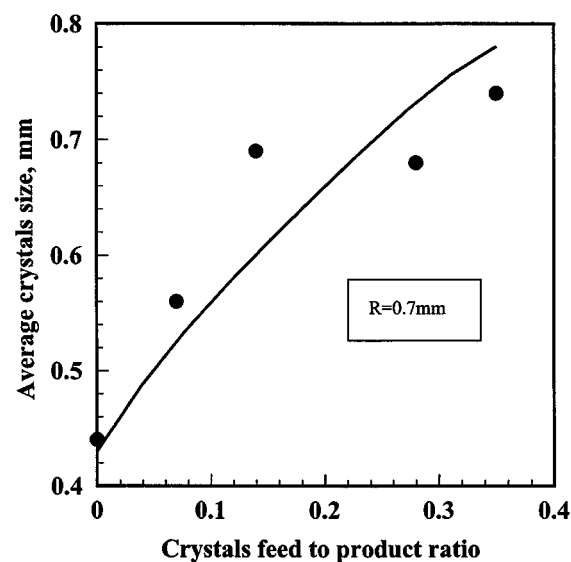


Figure 8. Effect of the relative crystals feed to product ratio on the average product crystal size.

The dots represent experimental data; the lines are calculated theoretical results.

size, it could be attributed to an experimental error, but the theoretical analysis, presented with the curved line, shows a similar trend.

By raising the crystals volume concentration within the crystallizer, the number of particles encountered is increased and, consequently, the rate of formation of the new crystallization nuclei B is increased. This, in turn, leads to the decrease of d , the average size of crystals. The precipitated mass at low crystal volume concentration is distributed between the formation of new nuclei and the increase of the average size of existing crystals d . Thus, a maximum value for the average size of crystals d can be explained as shown (Figure 5).

Effect of Suspension Circulation

The influence of the suspension circulation to magma volume ratio ω on the average size of crystals d , the rate of formation of new crystallization B , and the rate of growth crystals G are given in Figure 6. Increasing the ratio ω by almost 20% causes the rate of formation of new nuclei B to increase by about 200%. Increase in the rate of formation of new nuclei B leads to the decrease in the rate of crystals growth G by almost 20%, and, hence, leads to a decrease of the average size of product. The computed formation rates for new crystallization centers B , and average size of crystals d were in good agreement with the experimental values.

Effects of Crystals in Feed

The proposed crystal formation and growth model was compared to an actual experimental data of potassium chloride crystallization. In the case of circulation crystallization where the rate of discharge of fine particles $\chi = 0$, Eq. 27 can be rewritten

$$Q = kV \quad (33)$$

The rate k of crystals discharged from the crystallizer can be determined simply from the above relation. The solid-phase output rate- Q can be determined from the mass balance.

The rate of formation of new crystallization nuclei B was determined from measurements made on samples of the salt product. The output rate Q and the average crystal size d were found by evaluation of the experimental data with the aid of Eqs. 16 and 18.

The experimental conditions of the experiments in the crystallizer with crystals in the feed were: feed flow rate $0.33 \times 10^{-5} \text{ m}^3/\text{s}$, feed temperature $58\text{--}61^\circ\text{C}$, solution density $(1.199\text{--}1.201)10^3 \text{ kg/m}^3$, and temperature of the suspension in the crystallizer $28\text{--}32^\circ\text{C}$.

The results of the experimental investigations are given in Figures 7 and 8. Examination of these results shows that the size and the flow rate of the feed crystals have a significant influence on the size distribution function of the final product. Figure 7 shows the influence of the size of feed crystals R on the average crystal size of the product. The triangle on the left represents the results with no solids fed into the crystallizer. The circles represent experimental results for different sizes fed into the crystallizer, while the line represents the analysis presented here. In this set of experiments the ratio between the feed crystals and the product output was

0.14. It is clear from Figure 7 that, for $R < R^*$ ($R < 0.07 \times 10^{-3} \text{ m}$), the average size of crystals decreases. When $R > R^*$ with a rising size of the feed particles R , the average crystals size of the product becomes an increasing function of R ; this is in agreement with the theoretical results given above.

Figure 8 shows the influence of the relative crystals feed to product ratio q/Q on the average product crystal size. Again, the comparison of experimental data with the theory presented here is good.

Conclusions

The analytical analysis demonstrated in this article shows the influence of different crystallization parameters on the product-size distribution. Parameters checked by this approach were the rate of removal of fines from the circulation, the size and the relative flow rate of the feed crystals into the crystallizer and the concentration of crystals in the suspension and the suspension circulation to magma volume ratio. All these parameters show an influence on the product-size distribution; hence, they may be used in controlling the required size of the product. Experimental results are in good agreement with theoretical predictions presented here.

Acknowledgment

The research was supported by the Technion's fund for the promotion of research. Grigory Zelmanov acknowledges support in part by the Israeli Ministry of Absorption.

Notation

- B = nucleation rate, $1/\text{m}^3 \cdot \text{s}$
- $f(x)$ = size distribution function of crystals of size x , $1/\text{m}^4$
- l = number-average crystal size, m, mm
- x = crystal size, m, mm
- γ = shape factor
- $\mu(j)$ = j th moment of crystal distribution function
- φ = ratio of the flux of solid feed q over solid phase output rate Q
- φ_1 = ratio of the output rate of fine crystals Q_1 over solid phase output rate Q
- ω = suspension circulation to magma volume ratio, $1/\text{s}$

Literature Cited

- Eek, R. A., S. Dijkstra, and G. M. van Rosmalen, "Dynamic Modeling of Suspension Crystallizers, Using Experimental Data," *AIChE J.*, **41**, 571 (1995).
- Han, C. D., and R. Shinnar, "The Steady State Behavior of Crystallizers with Classified Product Removal," *AIChE J.*, **14**, 612 (1968).
- Hounslow, M. J., and E. J. W. Wynn, "Modeling Particulate Processes: Full Solutions and Short Cuts," *Comput. Chem. Eng.*, **16**, 411 (1992).
- Nauman, E. B., and T. T. Szabo, "Nonselective Fines Destruction in Recycle Crystallizers," *Chem. Eng. Prog. Symp. Ser.*, **67**, 108 (1971a).
- Nauman, E. B., "Selective Fines Destruction in Recycle Crystallizers," *Chem. Eng. Prog. Symp. Ser.*, **67**, 116 (1971b).
- Qiu, Y., and A. C. Rasmuson, "Estimation of Crystallization Kinetics from Batch Cooling Experiments," *AIChE J.*, **40**, 799 (1994).
- Randolph, A. D., and M. A. Larson, "Analysis and Techniques of Continuous Crystallization," *Academic Press*, London (1988).
- Rawlings, J. B., S. M. Miller, and W. R. Witkowski, "Model Identification and Control of Solution Crystallization Processes: A Review," *Ind. Eng. Chem. Res.*, **32**, 1275 (1993).
- Rawlings, J. B., and W. H. Ray, "Stability of Continuous Emulsion Polymerization Reactors: A Detail Model Analysis," *Chem. Eng. Sci.*, **42**, 2767 (1987a).

- Rawlings, J. B., and W. H. Ray, "Emulsion Polymerization Reactor Stability: Simplified Model Analysis," *AIChE J.*, **33**, 1663 (1987b).
- Rojkowski, Z. H., "Crystal Growth Rate Models and Similarity of Population Balances for Size-Dependent Growth Rate and for Constant Growth Rate Dispersion," *Chem. Eng. Sci.*, **48**, 1475 (1993).
- Saeman, W. C., "Crystal-Size Distribution in Mixed Suspensions," *AIChE J.*, **2**, 107 (1956).
- Tavare, N. S., *Industrial Crystallization. Process Simulation Analysis and Design*, Plenum, New York (1995).
- Todes, O. M., V. A. Seballo, and A. D. Golziker, "Bulk Crystallization from Solutions," *Metalurgia*, Leningrad (1984).
- Zelmanov, G., "Particle Dispersion Analysis during Salt Crystallization from Solution," PhD Thesis, Leningrad Univ. of Technology, USSR (1991).
- Zelmanov, G., "Particle Dispersion Analysis during Large-Scale Salt Crystallization from Solution," *Zhurnal Prikladnoi Khimii*, **61**, 1624 (1988).
- Zelmanov, G., E. Y. Tarat, and G. S. Cherkez, "Study of Controlled Vacuum Crystallization of Potassium Chloride," *Zhurnal Prikladnoi Khimii*, **52**, 1297 (1979).
- Wynn, E. J. W., and M. J. Hounslow, "Integral Population Balance Equations for Growth," *Chem. Eng. Sci.*, **52**, 733 (1996).

Manuscript received May 19, 1999, and revision received Jan. 6, 2000.